WHAT IS AN APPROPRIATE FACTOR OF SAFETY FOR LANDFILL COVER SLOPES?

C.N. LIU
THE UNIVERSITY OF TEXAS AT AUSTIN, USA
R.B. GILBERT
THE UNIVERSITY OF TEXAS AT AUSTIN, USA
R.S. THIEL
THIEL ENGINEERING, USA
S.G WRIGHT
THE UNIVERSITY OF TEXAS AT AUSTIN, USA

ABSTRACT

Factors of safety used for the design of embankment dams are not necessarily appropriate for the design of landfill covers. The level of uncertainty in the design of cover slopes may be greater than for embankment dams due to the lack of project-specific strength testing and the effect that small changes in water and gas pressures can have on stability. Laboratory shear tests are presented to illustrate the sources of uncertainty in interface strength for cover slopes. Sensitivity analyses are performed to highlight the importance of fluid pressure on the factor of safety. Finally, a simplified methodology is presented for selecting the appropriate factor of safety by considering design uncertainty and balancing costs and benefits.

INTRODUCTION

Landfill cover systems typically consist of a barrier layer overlain by a drainage layer, cover soil and vegetation and sometimes underlain by a gas collection or drainage layer. The individual components in the system include both soil and geosynthetic materials. Interfaces between individual components form potential sliding surfaces in the cover system (Fig. 1).

A limit equilibrium model is commonly used in practice to evaluate the stability of cover slopes. The factor of safety for static conditions is defined as the ratio of the available strength divided by the strength required for stability; which for an infinite slope is expressed by

$$FS = \frac{c' + (\gamma z \cos\alpha - u)\tan\phi'}{\gamma z \sin\alpha} \qquad (1)$$

where
FS = factor of safety
γ = unit weight of material in slope
u = fluid pressure in slope at interface of slippage
c' = effective stress failure envelope intercept for interface
ϕ' = effective stress failure envelope slope for interface
α = slope angle
z = depth below the ground surface for interface

Buttress loads at the toe of the slope and tensile reinforcement within the slope are not included in Eq.1 and will not be considered in this paper.

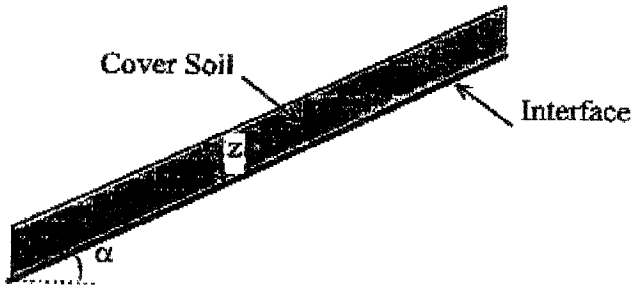

Fig. 1 Geometry of cover slope

A factor of safety of about 1.5 is commonly used for the design of slopes in landfill cover systems. This factor of safety has been adopted from the design of embankment dams. Experience over the past 50 years has indicated that this safety factor provides a reasonable balance between cost and performance for embankment dams. However, landfill cover slopes are not embankment dams. The magnitudes of uncertainty in design and the consequences of failure are different. In this paper, we will highlight and discuss the importance of these differences. We will also present a simplified methodology to obtain an appropriate factor of safety for a cover slope by (1) explicitly accounting for uncertainty in the performance and (2) considering the cost of failure.

INTERFACE SHEAR STRENGTH

An important difference between landfill cover slopes and embankment dams is the level of strength testing used in design. For a typical embankment dam, many project-specific strength tests are conducted. Conversely, it often happens that very little, if any, project-specific interface strength testing is performed in the design of a cover slope. The apparent rationale for the lack of testing with cover slopes is the perception that there is negligible uncertainty in interface strengths for geosynthetic materials because they are man-made. However, there are many sources of uncertainty in geosynthetic interface strengths, including (1) material variability, (2) accuracy of test methods, (3) the effects of moisture, and (4) post-peak strength reductions with displacement.

Variability in Geosynthetics. In order to study material variability for geosynthetics, the interface between a polyvinyl chloride (PVC) geomembrane and a woven geotextile was tested using a tilt table device. The geomembrane was a 40-mil thick, faille-finished PVC geomembrane manufactured by Watersaver Company, Inc. The non-faille finish side was placed against the geotextile. The woven geotextile was the upper component in the needle-punched geosynthetic clay liner (GCL) product manufactured by Bentomat®. Test specimens were 133 mm x 133 mm in size. The 600-mm long tilt table was raised at a rate of about 1° per minute. The angle at which observable sliding occurred was used to estimate the interface strength. Five tests each were performed at three normal stresses. For both the geotextile and the geomembrane, the individual test specimens were obtained from the same batch of material. The test results are shown on Fig. 2.

Variability in the interface strength tends to increase with increasing normal stress. A useful measure of this variability is the coefficient of variation (c.o.v.), which is equal to the standard deviation divided by the mean value at a given normal stress. The c.o.v. values are essentially constant with normal stress, and range from 1 to 2 percent.

Test results for a different batch of the woven geotextile at an approximate normal stress of 15 kPa are shown on Fig. 3. The variability between batches is more significant than the variability within a batch. The difference of the average-strength-to-normal-stress ratios between batches is about 5 percent. This result indicates that conducting repeated tests on material from a single batch will not capture fully the magnitude of material variability.

Including both intra- and inter-batch variability, the variability in the strength of this geosynthetic interface is still relatively small. For example, typical c.o.v. values for the strength of soils range from 10 to 30 percent. However, the variability of the geosynthetic interface strength cannot be neglected if only one specimen is tested at a single normal stress (a common practice for cover slopes). This single strength measurement, which would be used to design the slope, could easily be more than 5 percent different from the average measured strength for the interface.

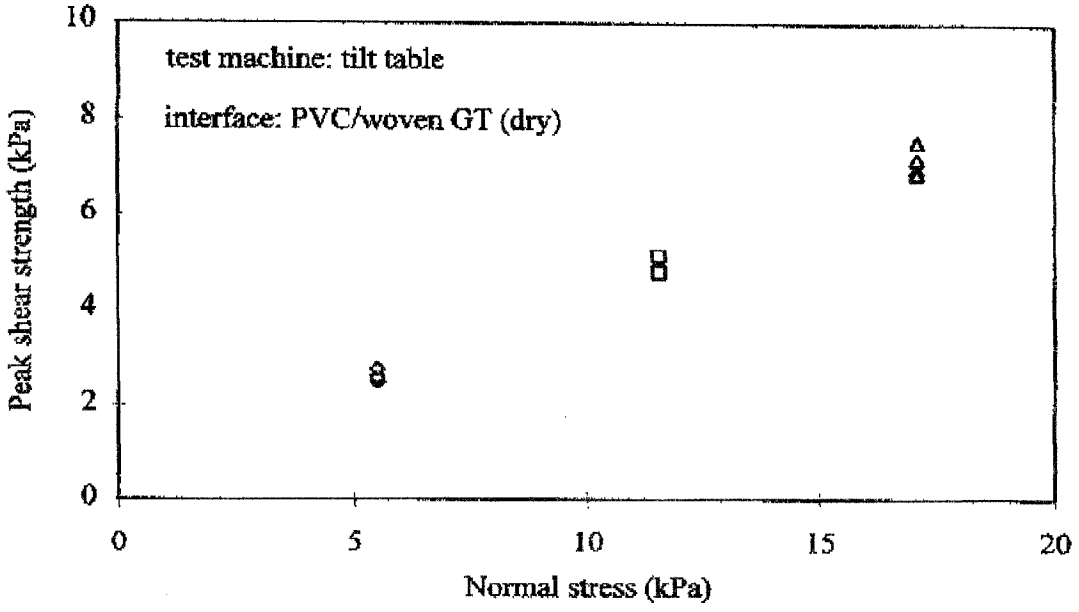

Fig. 2 Variability in peak interface strength

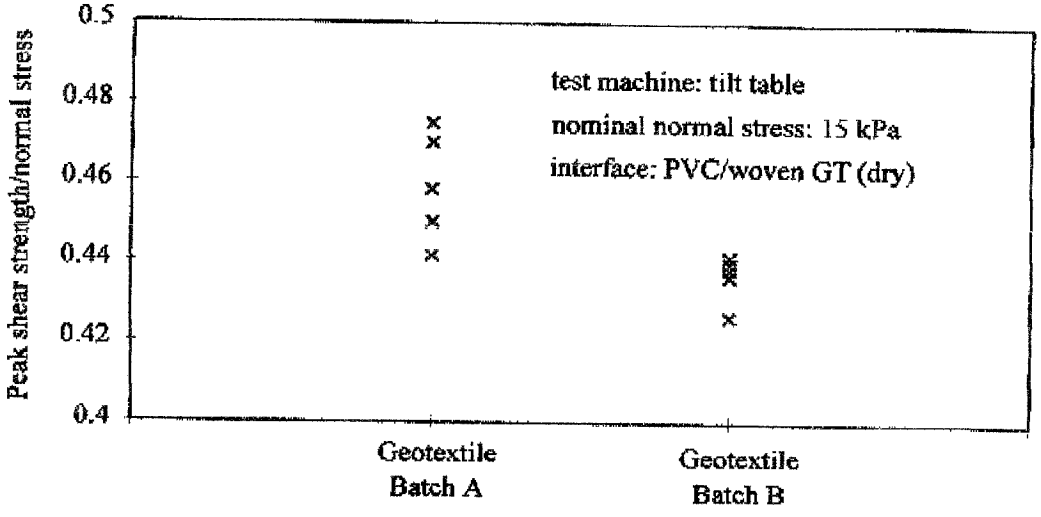

Fig. 3 Variability in peak interface strength between batches

Accuracy of Shear Strength Test Methods. Shear strength tests were performed on the woven geotextile/PVC geomembrane interface using four different devices: a direct shear box with a circular specimen 64 mm in diameter (Direct Shear #1); a direct shear box with a circular specimen 60 mm in diameter (Direct Shear #2); a double interface shear device with a square specimen 102 mm on a side (Double Interface Shear); and the tilt table with a 133 mm square specimen. In all cases, a comparable rate of shear equal to approximately 0.5 mm/min was used. Since the strength measured with the tilt table corresponds to the peak strength, the peak strengths for the other devices are used for comparison. From five to ten tests were conducted with each device to account for inter-device (or material) variability.

The test results are shown on Fig. 4. The variability between devices is significant. Surprisingly, there is a large discrepancy in results from the two direct shear boxes with similar specimen sizes; the average ratio of strength to normal stress from Direct Shear #2 was 87 percent of that for Direct Shear #1. The results from the double interface and tilt table devices were closer together than those from the direct shear boxes. In fact, the double interface shear device and the tilt table produced results that are comparable to the average result for the two direct shear boxes.

In order to further investigate the differences between different test methods, tests were performed at normal stresses ranging from 5 to 18 kPa for each test method. A linear failure envelope was fit through the test data using a least squares regression analysis, and the results are summarized in Table 1. The failure envelopes for the double interface and tilt table devices are similar, while that from the direct shear box is flatter. For these failure envelopes, the difference in strength at a given normal stress is as large as 10 percent. For example, the strengths at a normal stress of 5 kPa range from 2.19 to 2.39 kPa.

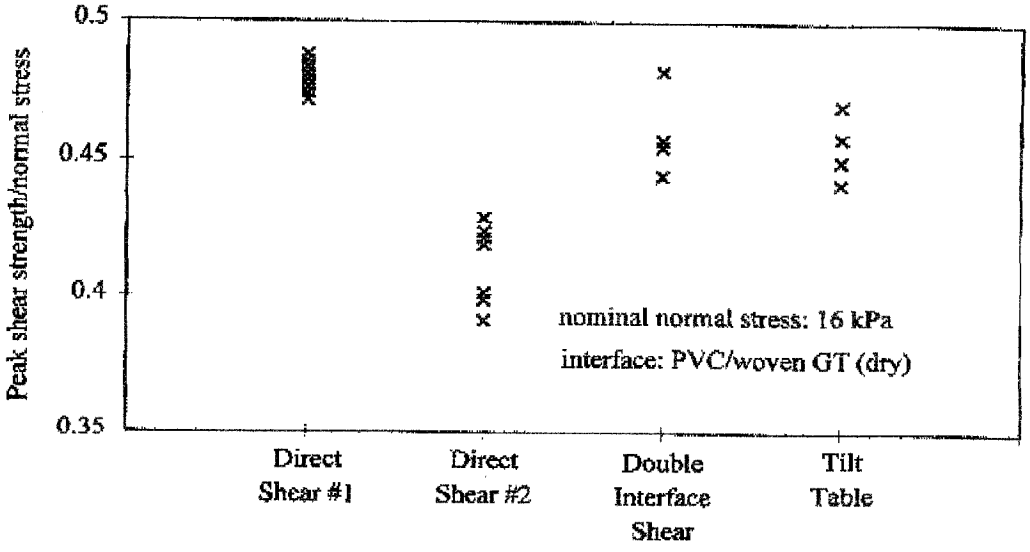

Fig. 4 Variability in peak interface shear strength between test devices

Table 1 Comparison of failure envelopes for different test devices

Test Method	Number of Tests	Intercept c' (kPa)	Slope ϕ' (°)	r^2
Direct Shear #1	15	0.45	21.2	0.99
Double Interface Shear	9	0.07	24.0	0.99
Tilt Table	15	0.08	22.9	1.00

Moisture Conditions. Moisture can lower the effective stress failure envelope for interfaces with geosynthetics. For example, the PVC geomembrane/woven geotextile interface strength decreases by more than 15 percent if it is submerged in water (Fig. 5). This strength reduction is not related to water pressure at the interface because the tests were run slowly enough to ensure complete drainage of the geotextile (based on its permittivity).

Moisture can also reduce the effective stress strength parameters for the interface between a PVC geomembrane and the woven geotextile of a geosynthetic clay liner (GCL) because hydrated bentonite from the GCL can extrude into the interface (Gilbert, et al. 1996). To investigate the effect of bentonite on the drained interface strength, tests were conducted on submerged interfaces in which bentonite was smeared on the woven geotextile at an areal density of 0.0002 g dry bentonite per mm^2. The rate used to raise the tilt table, about 1° per minute, was slow enough to ensure drained conditions for this thin layer of bentonite. The test results are shown in Fig. 5. Upper and lower bounds for the effective stress failure envelope are also given. The upper bound roughly corresponds to the dry, clean interface while the lower bound corresponds to the submerged, smeared interface. The lower bound strength is about 50 percent of the upper bound strength.

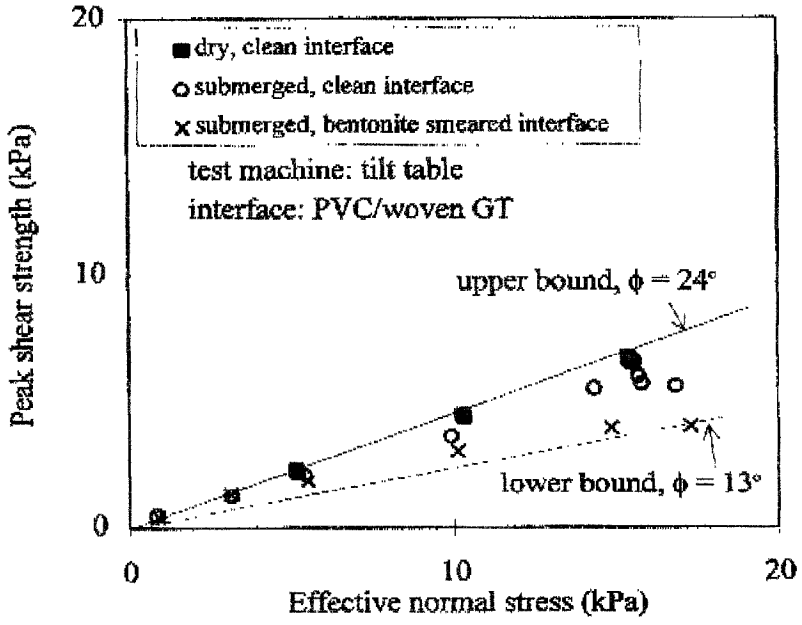

Fig. 5 Effect of moisture on effective stress failure envelope

Post-Peak Strength Reductions. Many interfaces with geosynthetics exhibit post-peak reductions in strength with displacement. A peak strength is mobilized at a small displacement (typically much less than 10 mm); the strength then decreases with further displacement, eventually approaching a residual value. For example, a plot of stress versus displacement for the submerged PVC geomembrane/woven geotextile interface with smeared bentonite is shown on Fig. 6. The bentonite was smeared on the woven geotextile at an areal density of 0.0002 g dry bentonite per mm^2. The test was performed using the double interface shear device, and the interface was sheared at a drained shear rate. The strength after large displacement is about 80 percent of the peak strength. Gilbert and Byrne (1996) and Stark et al. (1996) present data demonstrating that the residual strength for some geosynthetic interfaces is as small as 30 percent of the peak strength.

The ability to measure accurately the large-displacement or residual strength is affected by the test method and specimen size (Gilbert, et al. 1995). However, even if the peak and residual strengths for an interface are well established, uncertainty in the available strength in a cover slope (peak or residual) is a significant source of uncertainty in cover slope performance. Displacements during construction may be large enough to induce post-peak strength reductions. For example, displacements in a cover soil during construction were measured in thirteen, 10-m high cover slopes for a field test project (Scranton 1996). The measured displacements were greater than 25 mm on average. In addition, long-term deformation and creep may lead to strain softening.

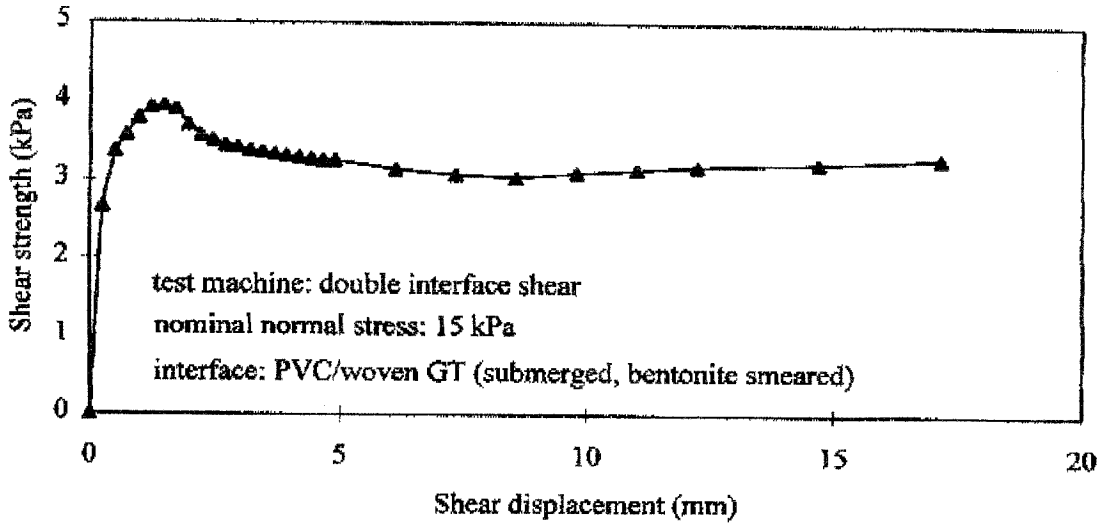

Fig. 6 Shear stress-displacement curve showing strain softening for a drained test

FLUID PRESSURE

Another difference between cover slopes and embankment dams is the effect that small changes in fluid pressure can have on the factor of safety. Because the overburden pressure on an interface in a cover system is typically small compared to that on the critical slip surface in an embankment dam, the factor of safety for a cover slope is more sensitive to a small change in fluid pressure. In order to demonstrate this sensitivity, the derivative of the factor of safety (Eq. 1) with respect to fluid pressure is given as follows

$$\frac{dFS}{du} = \frac{-\tan\phi'}{\gamma z \sin\alpha} \tag{2}$$

As the overburden pressure on the interface decreases (that is, as the depth of the interface, z, decreases), the factor of safety becomes more sensitive to fluid pressure (that is, the magnitude of the derivative dFS/du increases).

As an example of how sensitive the factor of safety is to fluid pressure for a cover slope, consider the cover slope shown on Fig. 7. The interface of concern for stability is that between the PVC geomembrane and the woven geotextile of the GCL (Figs. 5 and 6). Two sources of fluid pressure will be examined for this case: (1) gas pressure from the underlying waste and (2) pore water pressure due to a rapid change in the unit weight of the overlying cover soil if it becomes saturated during a rain storm.

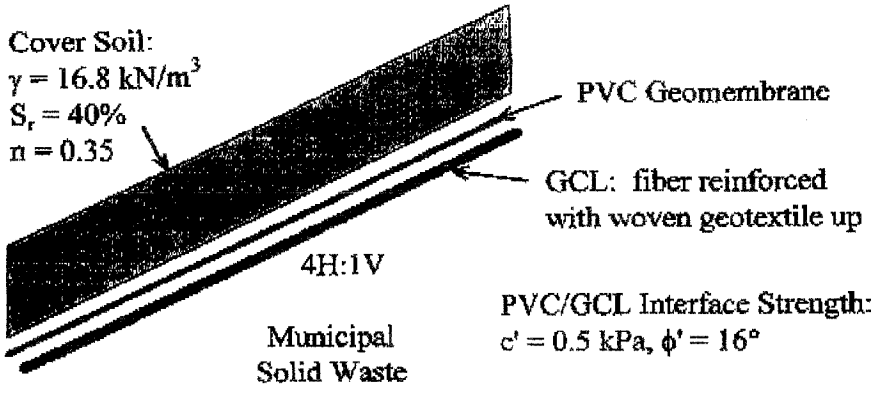

Fig. 7 Example cover slopes used for stability analyses

The magnitude of gas pressure at the base of a landfill cover is site specific, depending on a number of factors such as the waste composition and age, the moisture content of the waste, and the type and effectiveness of gas extraction systems. Average, ambient gas pressures for typical municipal solid waste landfills have been reported to be on the order of 1 kPa (Findikakis and Leckie 1979), while one of the authors (Thiel) has measured values ranging from 0 to 4 kPa below cover systems. The factor of safety for this slope is summarized in Table 2 for different gas pressure conditions. Two geometries are included: a temporary configuration during construction when a 0.3-m thick drainage layer is placed over the geomembrane and the final configuration when there is 0.9-m of cover soil over the geomembrane.

The results in Table 2 demonstrate two important points. First, a small increase in fluid pressure can have a large impact on the factor of safety. For both configurations, a 4 kPa gas pressure leads to a factor of safety less than one. For reference, a 4 kPa gas pressure corresponds to an equivalent water head of 0.4 m. Second, the factor of safety is more sensitive to fluid pressure for smaller overburden stresses. The factor of safety decreases from 1.56 to 0.62 for a 0.3-m thick cover due to a 4-kPa increase in gas pressure, while it only decreases from 1.29 to 0.97 for a 0.9-m thick cover.

Table 2 Effect of fluid pressure on the factor of safety

Case	γ (kN/m^3)	u (kPa)	FS for 0.3-m Cover (construction)	FS for 0.9-m Cover (post-construction)
No Fluid Pressure	16.8	0	1.56	1.29
Typical Gas Pressure	16.8	1	1.32	1.21
High Transient Gas Pressure	16.8	4	0.62	0.97
Rapid Increase in Cover Soil γ	18.8	0.6 (0.3-m cover) 1.7 (0.9-m cover)	1.39	1.15

Another potential source of fluid pressure at the interface is a rapid increase in the unit weight of the cover soil from rainfall infiltration. This increase in total normal stress at the interface will initially be carried by water pressure if the interface is saturated. Since the bentonite layer in the GCL will limit drainage below the woven geotextile, it may take days for this excess water pressure to dissipate; therefore, the effective normal stress and, thus, the strength, at the interface will not change during a storm event. However, the shear stress applied to the interface increases due to the increase in the weight of the cover soil. Hence, the factor of safety will temporarily decrease until either the cover soil dries back out or the excess water pressure at the interface dissipates. The effect of a rapid increase in the unit weight of the cover soil, assuming that cover soil saturation increases from 40 to 100%, is demonstrated in Table 2.

While this example has focused on the interface below the geomembrane, it is important to point out that water pressures at interfaces above the geomembrane will also be affected by infiltration. Therefore, the interface with the lowest factor of safety may actually vary with time depending on the magnitudes of fluid pressure at different interfaces within the cover system. Thiel and Stewart (1993), Giroud et al (1995) and Soong and Koerner (1995) address the fluid pressures that may develop above barrier layers from infiltration and seepage.

SO WHAT IS AN APPROPRIATE FACTOR OF SAFETY?

The intent of a factor of safety is to account for uncertainty in design. The actual factor of safety for a cover slope interface is not known due to uncertainty in the interface strength, the fluid pressure, the unit weight of soil above the interface and the constructed slope angle. By estimating values for these variables and then applying a factor of safety of about 1.5, designers hope that there is only a small chance that the actual factor of safety is less than one. However, there is a danger in blindly applying a safety factor of 1.5 without considering the probability of a slope failure. First, the probability may be unacceptably large, leading to unintended risk. Second, the probability may be unnecessarily small, leading to excessive cost. The objective of this section is to provide and demonstrate tools for evaluating the amount of uncertainty in the factor of safety, estimating the probability of a slope failure, and determining an appropriate factor of safety considering costs and benefits.

Uncertainty in the Factor of Safety. Uncertainty in the factor of safety for an interface arises from uncertainty in the individual design variables. The contribution of an individual variable to the overall uncertainty in the factor of safety depends on the (1) magnitude of uncertainty in the variable and (2) sensitivity of the factor of safety to the variable. Appendix A provides a simple tool for quantifying uncertainty in the factor of safety. Equations are given to estimate the mean factor of safety and the standard deviation in the factor of safety as a function of the means and coefficients of variation (c.o.v.) for all the variables in Eq. 1.

As an example, further analyses for the cover slope shown on Fig. 7 and analyzed in Table 2 (post-construction case with 0.9-m of cover soil) are presented in Table 3. Estimates of the c.o.v. for each variable are provided, and the partial derivatives of FS with respect to each variable are calculated (Appendix A). The soil unit weight and the fluid pressure at the interface are assumed to be positively

correlated since transient increases in γ may induce excess water pressure below the geomembrane. In addition, c' and $\tan\phi'$ are assumed to be negatively correlated from the linear regression analysis (that is, a larger slope on an envelope fit through the data would be associated with a smaller intercept).

The estimated mean factor of safety, μ_{FS}, is 1.21 from Eq. A.1, while the estimated standard deviation in the factor of safety, σ_{FS}, is 0.22 from Eq. A.2. In addition, a measure of the contribution of each variable to the overall uncertainty in the factor of safety is presented in Table 3. This uncertainty contribution factor is defined as follows

$$\text{Uncertainty Contribution Factor for X} = \frac{\sigma_{FS} - \sigma_{FS(\Omega_X=0)}}{\sigma_{FS}} \tag{3}$$

where X is a design variable and $\sigma_{FS(\Omega_X=0)}$ is the standard deviation of the factor of safety if there was no uncertainty in that particular variable. If a variable contributes little to the overall uncertainty in the factor of safety, then its uncertainty contribution factor will be near zero. Conversely, this factor will be near one for variables that contribute significantly to uncertainty in the factor of safety. The results in Table 3 show that uncertainty in the fluid pressure and failure envelope slope contribute most to uncertainty in the factor of safety. The failure envelope's slope ($\tan\phi'$) contributes because its c.o.v. is relatively large and the factor of safety is sensitive to this variable (its partial derivative is large). The fluid pressure contributes primarily because its c.o.v. is very large. While the slope angle's sensitivity is large, it makes a negligible contribution to uncertainty in the factor of safety because its c.o.v. is very small. It is noteworthy that uncertainty in the failure envelope's cohesion intercept contributes little to uncertainty in the factor of safety. This result is due to two factors. First, since the mean value for c' is small, the factor of safety is not very sensitive to changes in c' relative to the other variables. Second, the negative correlation between c' and $\tan\phi'$ dampens the effect of uncertainty in c' because smaller values of c' tend to be associated with larger values of $\tan\phi'$.

Table 3 Calculations to estimate uncertainty in the factor of safety

Variable X	Mean Value μ_X	c.o.v. Ω_X	$\frac{\partial FS}{(\partial X / \mu_X)}$	Uncertainty Contribution Factor
γ^*	16.8 kN/m^3	0.05	-0.06	0.0
$(c')^{**}$	0.5 kPa	0.20	0.14	0.0
u^*	1 kPa	1.0	-0.08	0.1
$\tan(\phi')^{**}$	tan16°	0.20	1.07	0.6
α	14°	0.03	-1.25	0.0

$^*\rho_{\gamma,u} = 0.5$; $^{**}\rho_{c',\tan(\phi')} = -0.5$

Reliability. The reliability of the interface is defined as the probability that the factor of safety will be greater than 1.0. Once μ_{FS} and σ_{FS} are calculated for a particular case, the reliability can be approximated as follows

$$\text{Reliability} = \text{Probability that FS} > 1 \cong \Phi\left(\frac{\mu_{FS} - 1}{\sigma_{FS}}\right) \tag{4}$$

where Φ is the standard normal function, which is tabulated in many statistics textbooks and available in most spreadsheet packages. In the previous example with $\mu_{FS} = 1.21$ and $\sigma_{FS} = 0.22$, the reliability is approximated by $\Phi[(1.21-1)/0.22] = 0.83$. Alternatively, the probability that the interface is not stable in this case is equal to 1-0.83, or 0.17.

In most design situations, multiple cases are analyzed. For example, four possible cases were analyzed for this interface in Table 2. The previous reliability calculations correspond to the case denoted "Typical Gas Pressures." Since each of the four cases could occur and there is a chance of instability associated with each case, the overall probability for the interface should account for all of these possibilities. The overall or total failure probability for an interface can be obtained as follows

$$\text{Total Failure Probability} = \sum_{\text{all cases}} (\text{Failure Probability for Each Case}) \times (\text{Likelihood of Case}) \tag{5}$$

As an example, Table 4 summarizes calculations of the total failure probability for this cover slope interface. The total failure probability, 0.18, is dominated by the failure probability for the typical gas pressure case since this is the most likely (or the most frequent) condition over the design life of the cover.

Table 4 Calculation of total failure probability for interface

Case	Failure Probability	Likelihood over Design Life	Total Failure Probability
No Fluid Pressure	0.10	0.2	0.10×0.2
Typical Gas Pressure	0.17	0.7	0.17×0.7
High Transient Gas Pressure	0.53	0.05	0.53×0.05
Rapid Increase in Cover Soil γ	0.26	0.05	0.26×0.05
			Σ = 0.18

Finally, there are multiple interfaces in most typical cover systems. Since slippage may occur along any of these interfaces, the reliability for the slope must account for all of the potential interfaces of sliding. A simple and conservative approximation for the probability of instability in the slope is to add the individual probabilities of failure for each interface

$$\text{Failure Probability for Slope} \cong \sum_{\text{all interfaces}} \text{Failure Probability for each Interface} \tag{6}$$

For example, there are three interfaces of concern in the cover system shown on Fig. 7: cover soil/PVC; PVC/GCL; and GCL/subgrade. If the total failure probabilities for the interfaces are 0.01, 0.18 and 0.05 respectively, then the probability of failure for this slope is 0.01 + 0.18 + 0.05 = 0.24. As the number of interfaces increases, the probability of slope failure will tend to increase. Also, interfaces with relatively small failure probabilities may have a negligible effect on the overall failure probability for the slope.

Appropriate Factor of Safety. An "appropriate" factor of safety is defined as one that provides an optimal balance of costs and benefits. For both embankment dams and cover slopes, the primary cost associated with a smaller factor of safety is a greater probability of slope failure. A simple model to capture the impact of this cost is the expected cost of failure

$$\text{Expected Cost of Failure} = C_F p_F \tag{7}$$

where C_F is the cost of a slope failure and p_F is the probability of a slope failure. As the mean factor of safety decreases, the probability of failure and, thus, the expected cost of failure increases.

In order to relate the mean factor of safety to the expected cost of failure, a "contour" plot of the failure probability versus the mean and standard deviation for the factor of safety is shown on Fig. 8. This plot corresponds to a single interface under a single design condition. Fig. 8 can be used to determine an appropriate factor of safety in several ways.

Many civil engineering systems, such as embankment dams, have lifetime failure probabilities on the order of 0.0001 to 0.001. If a comparable level of reliability is desired for a landfill cover system, then the required mean factor of safety can be determined from Fig. 8 as a function of the magnitude of uncertainty in the factor of safety. For example, a standard deviation in the factor of safety equal to 0.22 was obtained for the PVC/GCL interface shown on Fig. 7. The required factor of safety to achieve a failure probability between 0.0001 and 0.001 for this case is between 1.6 and 1.7 (Fig. 8). This required factor of safety is larger than that used in embankment dams because there is more uncertainty in the design of a typical cover slope due to a lack of strength testing and the sensitivity to small changes in fluid pressure. For example, Christian et al. (1994) obtained a standard deviation of 0.14 in the factor of safety for an embankment slope. Note that this standard deviation is consistent with a mean factor of safety of about 1.5 for an embankment dam. Therefore, a factor of safety greater than 1.5 would be appropriate for cover slopes if a failure probability of 0.0001 to 0.001 is desired.

However, it may not be reasonable to achieve the same level of reliability in a landfill cover system as for an embankment dam because the cost of failure is significantly smaller. The expected cost of failure (Eq. 7) incorporates information about both the probability and cost of failure. Consider a small cover slope with a cost of failure of about $100,000. If it is designed with a failure probability of 0.001, then the expected cost of failure is only $100, which is insignificant. In fact, even a failure probability as large as 0.01, giving an expected cost of failure equal to $1,000, may be acceptable. The corresponding mean factor of safety is about 1.5 in this case.

Finally, it is possible to reduce the uncertainty in the factor of safety for cover slopes by performing project-specific strength tests. If the target probability of failure is 0.01, then the mean factor of safety could be as small as 1.1 for a standard deviation of 0.05 in the factor of safety (Fig. 8).

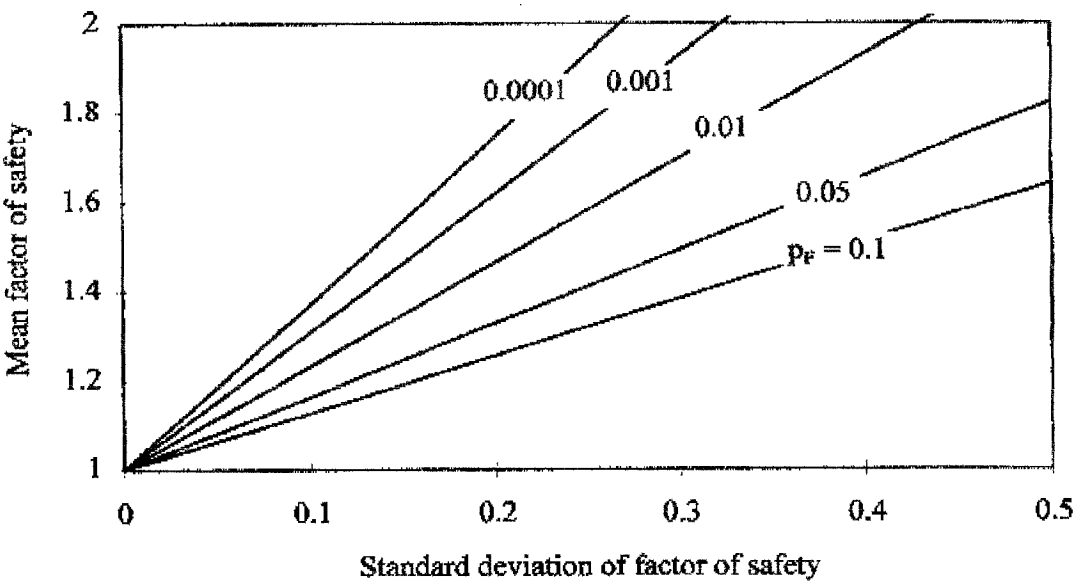

Fig. 8 Failure probability contours versus the mean and standard deviation of the factor of safety

CONCLUSIONS

In summary, selection of an appropriate factor of safety needs to be evaluated on a project-specific basis. Blind application of a factor of safety equal to 1.5 is not appropriate. An appropriate factor of safety for a cover slope could range from as small as 1.1 to greater than 1.5 depending on the amount of uncertainty and the cost of failure. The major factors affecting uncertainty in the performance of a cover slope are interface shear strengths and fluid pressures. Interface shear strengths contribute significant uncertainty if little project-specific testing is performed in design. We have demonstrated that the interface strength for geosynthetic materials can vary within and between batches, that test methods and test conditions can bias the results, and that the available strength depends on displacement due to strain softening. Fluid pressures contribute significant uncertainty because small changes in fluid pressure can have a significant effect on stability. Also, fluid pressures acting on cover system interfaces can include both water and gas pressures. Finally, we have provided a set of practical tools for quantifying uncertainty in the factor of safety, estimating the reliability of a cover slope, and ultimately selecting an appropriate factor of safety for design.

REFERENCES

Christian, J.T., Ladd, C.C., and Baecher, G.B., (1994) "Reliability applied to slope stability analysis", Journal of Geotechnical Engineering, ASCE, Vol. 120, No. 12, pp. 2180-2207.

Gilbert, R.B. and Byrne, R.J., (1996) "Strain-softening behavior of waste containment system interfaces", Geosynthetics International, Vol. 3, No. 2, pp. 2-23.

Gilbert, R.B., Fernandez, F.F. and Horsfield, D.W., (1996) "Shear strength of a reinforced geosynthetic clay liner", Journal of Geotechnical Engineering, ASCE, Vol. 122, No. 4, pp. 259-266.

Gilbert, R.B., Liu, C.N., Wright, S.G. and Trautwein, S.J., (1995) "A double shear test method for measuring interface strength", Geosynthetics '95 Conference Proceedings, Vol. 3, pp. 1017-1029.

Giroud, J.P., Bachus, R.C., and Bonaparte, R., (1995) "Influence of water flow on the stability of geosynthetic-soil layered systems in slopes", Geosynthetics International, IFAI, Vol. 2, No. 6, pp. 1149-1180.

Findikakis, A.N. and Leckie, J.O., (1979) "Numerical simulation of gas flow in sanitary landfills", Division of Environmental Engineering, ASCE, Vol. 105, No. 5, pp. 927-945.

Scranton, H.B., (1996) "Field performance of sloping test plots containing geosynthetic clay liners", Master Thesis, University of Texas at Austin, 206p.

Soong T.Y. and Koerner, R.M., (1995) "Seepage induced slope instability", Proceedings of the 9th GRI Conference, pp. 235-255.

Stark, T.D., Williamson, T.A., and Eid, H.T., (1996) "HDPE geomembrane/geotextile interface shear strength", Journal of Geotechnical Engineering, ASCE, Vol. 122, No. 3, pp. 197-203.

Thiel, R.S. and Steward, M.G., (1993) "Geosynthetic landfill cover design methodology and construction experience in the Pacific Northwest", Geosynthetics '93 Conference Proceedings, Vol. 3, pp. 1131-1144.

APPENDIX A. FIRST-ORDER APPROXIMATIONS FOR THE MEAN AND STANDARD DEVIATION OF THE FACTOR OF SAFETY

The mean or expected factor of safety can be estimated as follows

$$\mu_{FS} \cong \frac{\left[\mu_\gamma z\cos(\mu_\alpha) - \mu_u\right]\mu_{\tan\phi'} + \mu_{c'}}{\mu_\gamma z\sin(\mu_\alpha)} \qquad \text{(A.1)}$$

where μ indicates the mean (or "best guess") value for a parameter. Therefore, the mean value for FS is simply estimated from Eq. 1 by using the mean value for each parameter. Likewise, the standard deviation in FS can be estimated as follows

$$\sigma_{FS}^2 \cong \left(\frac{\partial FS}{\partial \gamma / \mu_\gamma}\right)^2 \Omega_\gamma^2 + \left(\frac{\partial FS}{\partial c'/\mu_{c'}}\right)^2 \Omega_{c'}^2 + \left(\frac{\partial FS}{\partial u / \mu_u}\right)^2 \Omega_u^2 + \left(\frac{\partial FS}{\partial \tan(\phi')/\mu_{\tan(\phi')}}\right)^2 \Omega_{\tan(\phi')}^2$$
$$+ \left(\frac{\partial FS}{\partial \alpha / \mu_\alpha}\right)^2 \Omega_\alpha^2 + 2\left(\frac{\partial FS}{\partial \gamma / \mu_\gamma}\right)\left(\frac{\partial FS}{\partial u / \mu_u}\right)\rho_{\gamma,u}\Omega_\gamma\Omega_u \qquad \text{(A.2)}$$
$$+ 2\left(\frac{\partial FS}{\partial c'/\mu_{c'}}\right)\left(\frac{\partial FS}{\partial \tan(\phi')/\mu_{\tan(\phi')}}\right)\rho_{c',\tan(\phi')}\Omega_{c'}\Omega_{\tan(\phi')}$$

where σ_{FS} is the standard deviation for FS, Ω indicates the coefficient of variation for a parameter (the standard deviation divided by the mean), ρ is the correlation coefficient between two parameters ($\rho_{\gamma,u}$ will tend to be positive since an increase in infiltration will increase both the unit weight and the pore water pressure, while $\rho_{c',\tan(\phi')}$ will tend to be negative since c' and tan(ϕ') are negatively correlated in a conventional regression analysis), and the partial derivatives of FS with respect to each parameter are evaluated at the mean values as follows

$$\frac{\partial FS}{\partial \gamma / \mu_\gamma} = \frac{1}{z\sin(\mu_\alpha)}\left(\frac{\mu_u}{\mu_\gamma}\mu_{\tan(\phi')} - \frac{\mu_{c'}}{\mu_\gamma}\right)$$

$$\frac{\partial FS}{\partial c'/\mu_{c'}} = \frac{\mu_{c'}}{\mu_\gamma z\sin(\mu_\alpha)}$$

$$\frac{\partial FS}{\partial u / \mu_u} = \frac{-\mu_u\mu_{\tan(\phi')}}{\mu_\gamma z\sin(\mu_\alpha)} \qquad \text{(A.3)}$$

$$\frac{\partial FS}{\partial \tan(\phi')/\mu_{\tan(\phi')}} = \frac{\left[\mu_\gamma z\cos(\mu_\alpha) - \mu_u\right]\mu_{\tan(\phi')}}{\mu_\gamma z\sin(\mu_\alpha)}$$

$$\frac{\partial FS}{\partial \alpha / \mu_\alpha} = \frac{\mu_\alpha}{\mu_\gamma z\sin(\mu_\alpha)}\left[\frac{-\mu_\gamma z\mu_{\tan(\phi')} + \mu_u\mu_{\tan(\phi')}\cos(\mu_\alpha) - \mu_{c'}\cos(\mu_\alpha)}{\sin(\mu_\alpha)}\right]$$

These derivatives indicate the change in FS for a percentage change in a parameter about its mean value. Therefore, they are useful measures of the sensitivity of FS to the various parameters.